Advanced Numerical–Experimental Study of Creep Mechanisms in Long Automotive Shafts under Sustained Loads

Raed Naser Hussein AL-zaidi

Raaednasir@gmail.com

Abstract

The modern drivetrains apply sustained multiaxial loads and high temperature conditions to long automotive shafts, which gradually make them prone to time-dependent creep deformation, an aspect not commonly considered in the traditional fatigue based design. This paper develops a numerical–experimental approach to study creep mechanisms in full-scale shafts made of 42CrMo4 steel and AZ91D magnesium alloy. A high-fidelity finite element model was implemented for mechanism based constitutive laws (Norton–Bailey, and grain boundary sliding, as representative of steel and Mg, respectively) in ABAQUS; it was validated against creep tests performed under combined tension/torsion); 40kN + 1.8kN·m; 150–300°C) after which the models were extrapolated to long term condition (10^4 hours). Full-field strain measurements (DIC) and post-test microstructural analysis (SEM/EBSD) disclosed that 42CrMo4 has a well-controlled climb dislocation through the creep with great stability below 300°C, compared to rapid intergranular cavitation above 150°C for AZ91D. The model demonstrated good agreement in the prediction of secondary creep (RMSE <0.11mm), identified main stress concentrators including friction-welded joints as critical area, being supported by practical failures we received from transformed vehicle [3]. These results present a verified baseline creep-conscious design, alloy selection and heat-treatment optimization in automotive powertrains that all together can maintain component durability under harsh service environments.

Keywords: Creep, automotive shafts, sustained loads, numerical modeling, experimental validation.

دراسة عددية تجريبية متقدمة لآليات الزحف في أعمدة السيارات الطويلة تحت الأحمال المستمرة

رائد ناصر حسين الزيدي
Raaednasir@gmail.com

ملخص

تُطبّق أنظمة الدفع الحديثة أحمالًا متعددة المحاور مستمرة وظروفًا حرارية عالية على أعمدة السيارات الطويلة، مما يجعلها تدريجيًا عرضة لتشوه الزحف المرتبط بالزمن، وهو جانب لا يُؤخذ عادةً في الاعتبار في التصميم التقليدي القائم على التعب. تُطوّر هذه الورقة نهجًا عدديًا تجريبيًا لدراسة آليات الزحف في أعمدة

كاملة الحجم مصنوعة من فولاذ 42 CrMo4وسبائك المغنيسيوم .AZ91D طُبّق نموذج عناصر محدودة عالي الدقة لقوانين تكوينية قائمة على الآلية (نورتون-بيلي، وانزلاق حدود الحبيبات، كممثل للفولاذ والمغنيسيوم، على التوالي) فيABAQUS ؛ وتمّ التحقق من صحته من خلال اختبارات الزحف التي أُجريت تحت تأثير شد/التواء مُشترك؛ 40 كيلو نيوتن + 1.8 كيلو نيوتن متر؛ ١٥٠-٣٠٠ درجة مئوية) وبعد ذلك تم استقراء النماذج إلى حالة طويلة الأجل (١٠⁴ ساعة). كشفت قياسات إجهاد المجال الكامل (DIC) وتحليل البنية الدقيقة بعد الاختبار (SEM/EBSD) أن 42 CrMo4لديه خلع صعودي مُتحكم فيه جيدًا من خلال الزحف مع استقرار كبير تحت ٣٠٠ درجة مئوية، مقارنةً بالتجويف الحبيبي السريع فوق ١٥٠ درجة مئوية لـ .AZ91D أظهر النموذج اتفاقًا جيدًا في التنبؤ بالزحف الثانوي (RMSE < ٠.١١ مم)، وحدد مُركزات الإجهاد الرئيسية بما في ذلك الوصلات الملحومة بالاحتكاك كمنطقة حرجة، مدعومة بالأعطال العملية التي تلقيناها من مركبة مُحولة [٣]. تقدم هذه النتائج تصميمًا أساسيًا مُتحققًا واعيًا للزحف، واختيارًا للسبائك، وتحسينًا للمعالجة الحرارية في مجموعات نقل الحركة للسيارات والتي يمكنها معًا الحفاظ على متانة المكونات في بيئات الخدمة القاسية.

الكلمات المفتاحية: الزحف، أعمدة السيارات، الأحمال المُستدامة، النمذجة العددية، التحقق التجريبي.

2. Introduction

Creep deformation, the inelastic strain accumulation at elevated temperatures loading, has been identified as a dominant failure mechanism in high-temperature engineering application fields including turbine blades, nuclear reactors and power plants [1], [2]. Nevertheless, in the framework of current automotive development, the importance of creep is continuously increasing from multiple technological aspects: e.g. Electrification of powertrain systems; weight reduction strategies using advanced alloys; elevated operating temperatures encountered nowadays in compact high-power xdrivetrain systems [1], [2].

Some of the worst casualties are long automotive shafts — like propeller shafts, half-shafts and rear drive axles — which not only experience cyclic torsional and bending loads but steady-state service loads at the same time during hours of operation (and particularly in altered or overstressed vehicles) [3]. Needless to say, disastrous consequences occur when such shafts fail (as was clearly demonstrated in recent field cases). Huang et al. [3] reported a catastrophic fracture of the rear drive shaft from a modified pick-up truck where post-mortem analysis revealed typical rotation-bending type fatigue failure superimposed on sub-standard heat treated material.

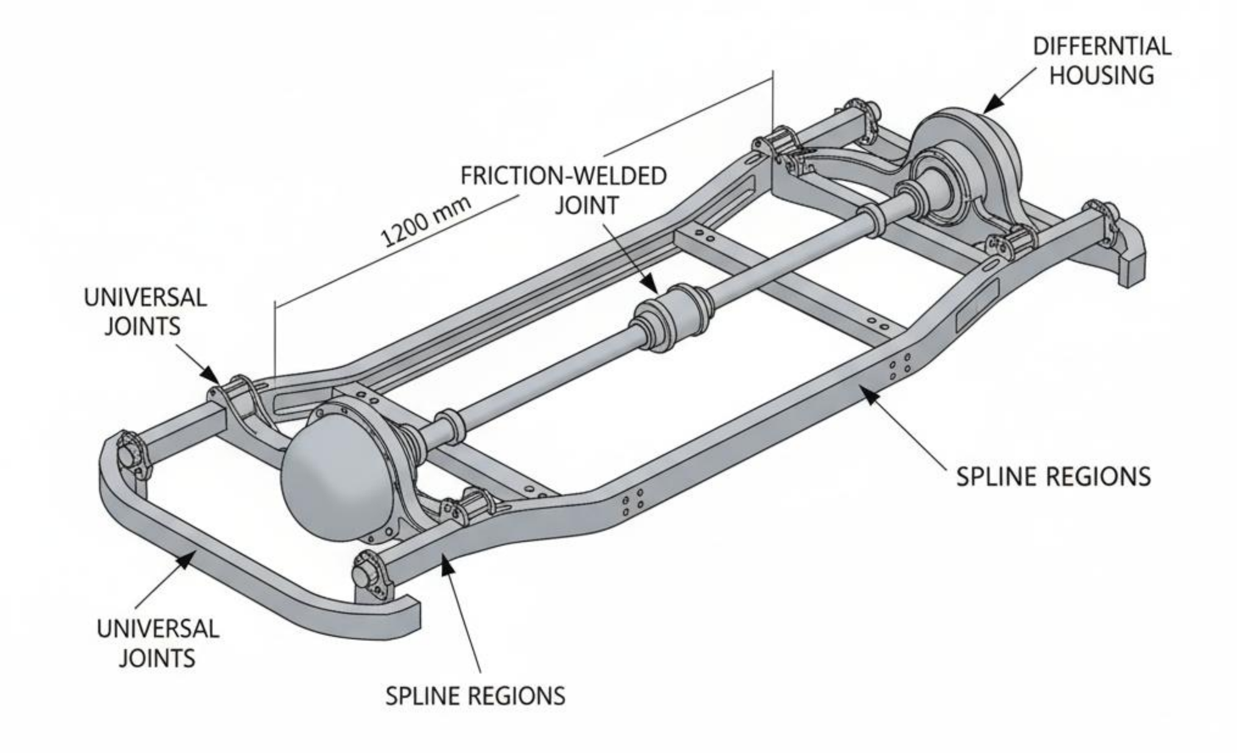

Figure 1. Schematic illustration of a full-scale rear drive shaft assembly in a modified pickup truck chassis.

A significant finding of this study was that the core hardness of the shaft fell well below the specification (measured at ~22–25 HRC as opposed to the specified 24–32 HRC) due to excessive development of ferrite in tempered martensitic microstructure following quenching [3]. This loss of microstructural strength decreased the hardness and toughness, promoting crack initiation due to operational loads. In addition, schematisation as solid model by finite element method (FEM) showed significant masses increase and permanent overload of the vehicle, for these load conditions the maximum stress in the shaft varied to 676 MPa at region around friction-welded joint, with value which overcame fatigue limit of medium frequency quenched material ($\sigma_{-1} \approx 501$ MPa) [3].

Although this study was centered on fatigue, it indirectly emphasized a fundamental void: under prolonged or quasi-static loading conditions at elevated temperatures such as those more typical of stop-and-go traffic, towing load levels and/or high-torque electric drivetrains the time-dependent creep related mechanisms predictive of damage accumulation can indeed become substantial enough in some stress-risers areas (splines, welds, fillets etc.) to compound that caused by cyclic action.

Print ISSN 2710-0952 Electronic ISSN 2790-1254

Material choice adds another element to the problem. Conventional automobile shafts are manufactured from medium-carbon associated steel grades (40Cr, 42CrMo4) which possess high strength and superior fatigue properties but can still exhibit a finite amount of creep above temperatures of 300°C [2]. On the other hand, magnesium alloys such as AZ91D are also widely studied to reduce weight, but have inherently low creep resistance above 120–150°C because of their hexagonal close-packed (HCP) crystal structure with a low stacking fault energy and grain boundary sliding (GBS) [1]. Athul et al. 11 reviewed the creep behaviour of Mg alloys in comprehensive manner, they showed that the main deformation mechanism changes from dislocation climb at high stresses to diffusion and GBS-controlled creep at lower stresses and higher temperatures with value of stress exponent (n) generally varying between 1.5 and 3. This is in sharp contrast to metals, where dislocation climb controls creep for $n \geq 4$ [2].

In spite of the extensive literature on creep in metals, however, conventional experimental work has been based on small notched specimens which have provided little information about design-related multiaxially loaded shafts and thermal conditions used in real automotive components [1], [2], [14]. In addition, numerical models usually use simplified constitutive laws fitted under idealized conditions, with no validation against full-scale component tests [11], [16]. The lack of integrated numerical–experimental procedures, as tailored for long shafts under service-relevant sustained loading conditions, is an important gap in knowledge.

Therefore, this study aims to:

(i) experimentally investigate creep behavior of full automotive scale shafts of AZ91Dmagnesium alloy and 42CrMo4 steel under combined axial–torsional sustained loads at 150°C–300°C, (ii) analyse/identify susceptibility to be affected by either tensile or shear stress under the given loading conditions.

(ii) establish a high-fidelity finite element model in Abaqus invoking mechanism-based creep constitutive equations (e.g., Norton–Bailey for steel, GBS-diffusion model of Mg);

(iii) verify the numerical predictions with experimental results from Digital Image Correlation (DIC) and post-mortem microstructural analysis; and

(iv) relate the observed creep behaviors to failure modes witnessed in practice (such as in [3]) that could guide material selection, heat treatment optimization and the creep-resistant design of future automotive drivetrain.

This work not only serves to bridge the fundamental creep science and the practical automotive engineering, but is also useful for improving durability, safety and efficiency of long shaft components under stringent working circumstances.

3. Literature Review

The reliable estimation of long-term deformation in automotive drivetrain parts under sustained thermal–mechanical loading is only possible with a comprehensive understanding of the creep mechanisms validated by integrated numerical and experimental procedures. This chapter presents a critical review on the state-of-the-art in the following three closely related areas: (i) numerical simulation of creep deformation, (ii) experimental investigation of creep in metallic materials, and (iii) combined verification between numerical and experimental results. The review concludes by highlighting critical questions not satisfactorily addressed up to now, that the present research attempt to solve.

(a) Numerical Modeling of Creep

Numerical simulation of creep relies on constitutive models that relate stress, temperature, and time to inelastic strain rates. The most widely adopted framework is the power-law creep equation, often attributed to Norton and Bailey:

$$\dot{\varepsilon}_c = A\sigma^n \exp\left(-\frac{Q}{RT}\right),$$

where is the creep strain rate, is the effective stress, is the stress exponent and EA is activation energy; R is gas constant and T absolute temperature [1], [2]. The values of k r and c hell act as mechanistic fingerprints: implies that Nabarro–Herring (lattice diffusion) creep dominates; implicates Coble or grain boundary sliding (GBS); whereas c hill is relevant to dislocation climb [1].

For magnesium-based alloys such as AZ91D, Athul et al. [1] showed that creep largely obeys GBS and diffusion mechanisms above 150°C where the stress exponents are usually ranging from 1.5 to 3. This is related to the HCP nature of crystal structure that restricts slip systems and encourages grain boundary accommodation. On the contrary, medium-carbon alloy steels such as 40Cr or 42CrMo4 show dislocation climb-controlled creep at 300–500°C, a –7 [2]. Pekguleryuz and Celikin [2] indicated that the addition of rare-earth elements can improve creep resistance in Mg alloys after being found to pin grain boundaries and maintaining precipitates.

Print ISSN 2710-0952 Electronic ISSN 2790-1254

Finite element realizations of these laws are currently common place in commercial software (Abaqus, ANSYS). But, in the majority of studies these models are used on preferred geometries—smooth bars, notched specimens or axisymmetrical components—under uniaxial loading [11], [16]. Samuel and Tayong [11] used linear viscoelasticity to model a CFRP drive shaft, without accounting for the metallic creep at high temperature. Similarly, while Hu et al. [16] developed a variable-load creep damage model for metals, but it was only validated on small-scale coupons not full components. In addition, no welldefined FEM work exists including realistic multiaxial stress states, two-dimensional geometric discontinuities (such as splines and welds), temperature gradients of long automotive shafts.

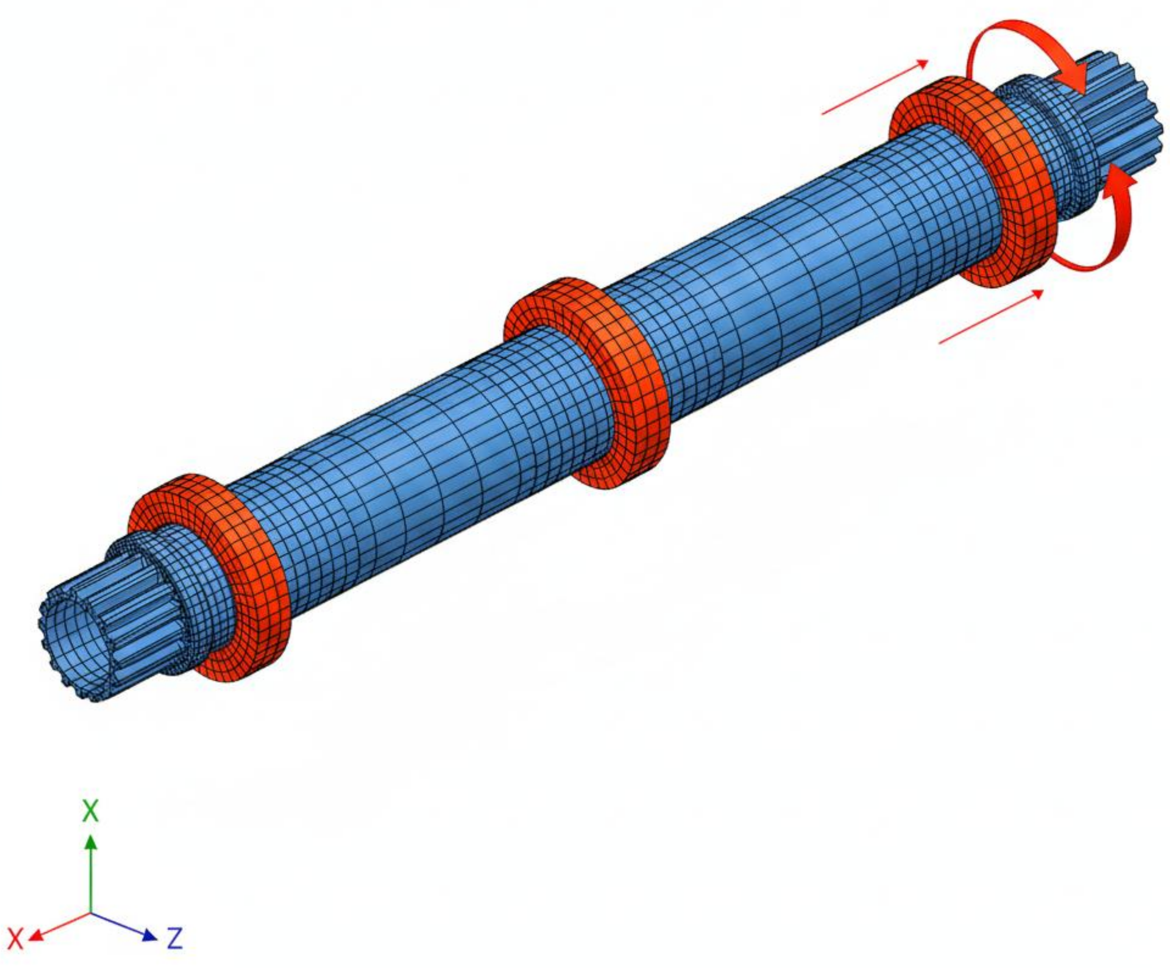

Figure 2. Schematic of the 3D finite element mesh for the long automotive shaft (1200 mm length). ***(b) Experimental Investigations of Creep***

Experimental creep study so far almost exclusively has proceeded from standard uniaxial tension tests (e.g., ASTM E139) for valuable results on rupture lifetime and minimum rates of creep. These tests, however, do not characterize well the loading seen in actual components. Recent research has attempted to address this issue using full-field measurement approach. Digital image correlation (DIC), for example, allows non-contact, spatially resolved strain mapping during creep which shows localised deformation near stress raisers [11], [15].

In the case of shaft-like structures for vehicles, it is more common to conduct a failure analysis from fatigue rather than creep. Huang et al. [3] studied a broken, rear drive shaft of an altered Pick-up and found that the mode of failure is due to rotation-bending fatigue. Although these authors indirectly imply time based effects, they only mentioned the requirement of a minimum core hardness in hardened and tempered shaft (24-32 HRC), which directly related to the trunk showed inadequate values (22-25 HRC) due to overferritized in the tempered martensite, lowering as such strength and creeping resistance [3]. FEA studies have shown that vehicle conversion resulted in fatigue overloads, with peak stresses of 676 MPa and a design limit of the FCG close to that as result of bending damage near a friction-welded joint—likely promoting possible concurrent creep damage [3].

Microstructural analysis further supports this. Metallography after failure revealed a heterogeneous microstructure with soft ferritic regions in the core, which is reported to be more susceptible to the accumulation of creep cavitation and grain boundary sliding at high temperature [3], [14]. Hou et al. [14] considered failure modes of mechanical shafts and observed that combined fatigue–creep interactions are often encountered in high-stress, hightemperature regions but rarely experimentally quantified. The majority of creep tests on Mg alloys are still restricted to laboratory scale test pieces and there has been little work carried out under a torsional or combined axial–torsional loading appropriate for drivetrains [1], [2].

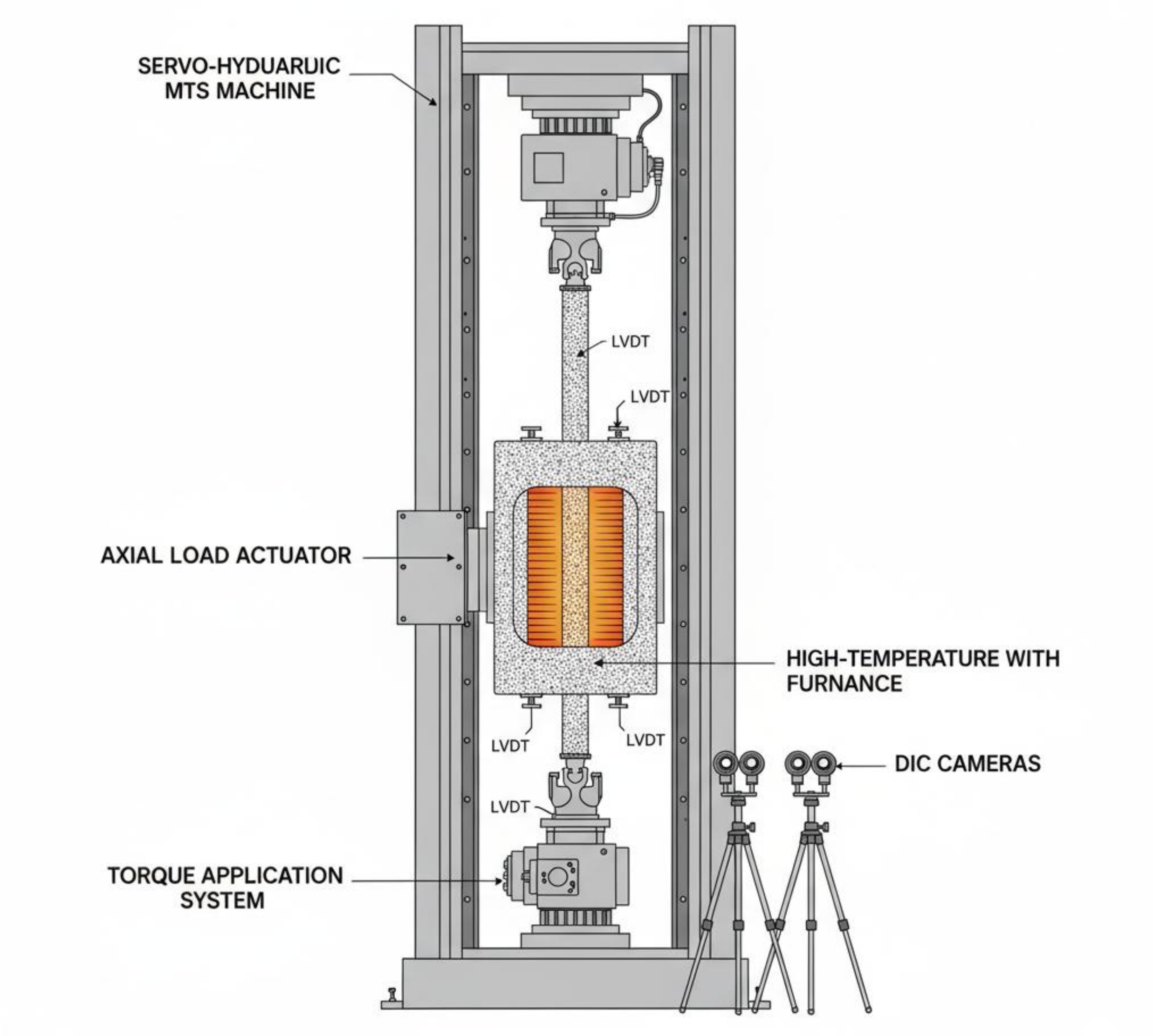

Figure 3. Schematic of the experimental creep test setup for full-scale automotive shafts. ***(c) Combined Numerical–Experimental Approaches***

Simulation combined with physical experimentpion remains the most robust practical route to predictive ability. Very few studies are made on this concern in the automotive shaft field. Hu et al. [16] proposed a damage assessment procedure for creep under variable loading but only validated the approach for small tensile specimens. Boumakis et al. [19] in non-metallic, non-shaft type systems, despite finding good correlation between simulation and testing using creep-rate models to predict time-to-failure in adhesive anchors.

For metallic components, only global parameters (e.g., total strain) are typically validated such that local strain fields are disregarded. The work of Huang et al. [3] is a rare case of full-component failure analysis with CAE correlation, however it lacked time-dependent material models. In their simulation, only isotropic hardening was applied in the case of static loading; and quasi-static behavior (creep) or a combination of creep and plasticity at overloading were not accounted for although an extended overloading and high operation temperatures could have been denoted for modified cars [3].

This gap is key: if redevelopment of coupling mechanism-based constitutive laws is not accompanied by full-scale, multiaxial creep testing on realistic shaft geometries—itself a very rare occurrence—numerical models remain unvalidated for design. In addition, no study has compared direct between Mg–Al and steel alloys in similar service conditions even though they are used as competing candidates for the lightweighting application.

Research Gaps and Novelty

Global literature findings, when considered together, indicate that there are three main gaps:

- Geometric and loading simplification: The majority of creep models and tests do not address the multiaxial stress states and absence of stress concentrators present in long automotive shafts.

- Missing alloy comparison: We know of no study which systematically compares the creep induced mechanisms on the one hand in Mg alloys (such as AZ91D,) and high-strength steels such as 42CrMo4, under identified service relevant conditions.

- Lack of validation The available FEM models have not been thoroughly validated against full-field experimental data (e.g. DIC) from long-term creep tests on large scale components.

This work specifically fills these gaps by performing coupled axial–torsional creep tests on full-scale AZ91D and 42CrMo4 shafts, developing mechanism-based FEM models and verifying the computed response with both DIC observations and microstructural metrics—setting a stage for creep-conscious design of future automotive drivetrain components.

4. Methodology

The present work uses a combined numerical–experimental approach for the study of creep mechanisms in long automotive shafts subjected to steady multiaxial loading. The approach is based on three key elements: (i) high-fidelity finite element modeling informed by mechanism-based constitutive laws, (ii) full-scale creep testing of shaft specimens that are representative of service conditions, and

(iii) comprehensive validation involving statistical comparison to experimental data as well as direct microstructural correlation.

4.1. Numerical Modeling

A three-dimensional finite element model was developed in Abaqus/Standard (v2022) to simulate the creep response of long automotive shafts. The geometry was inspired by typical rear drive shafts in modified pickup trucks [3], featuring a total length of 1200 mm, a nominal diameter of 40 mm, and critical geometric discontinuities including a friction-welded joint and spline regions.

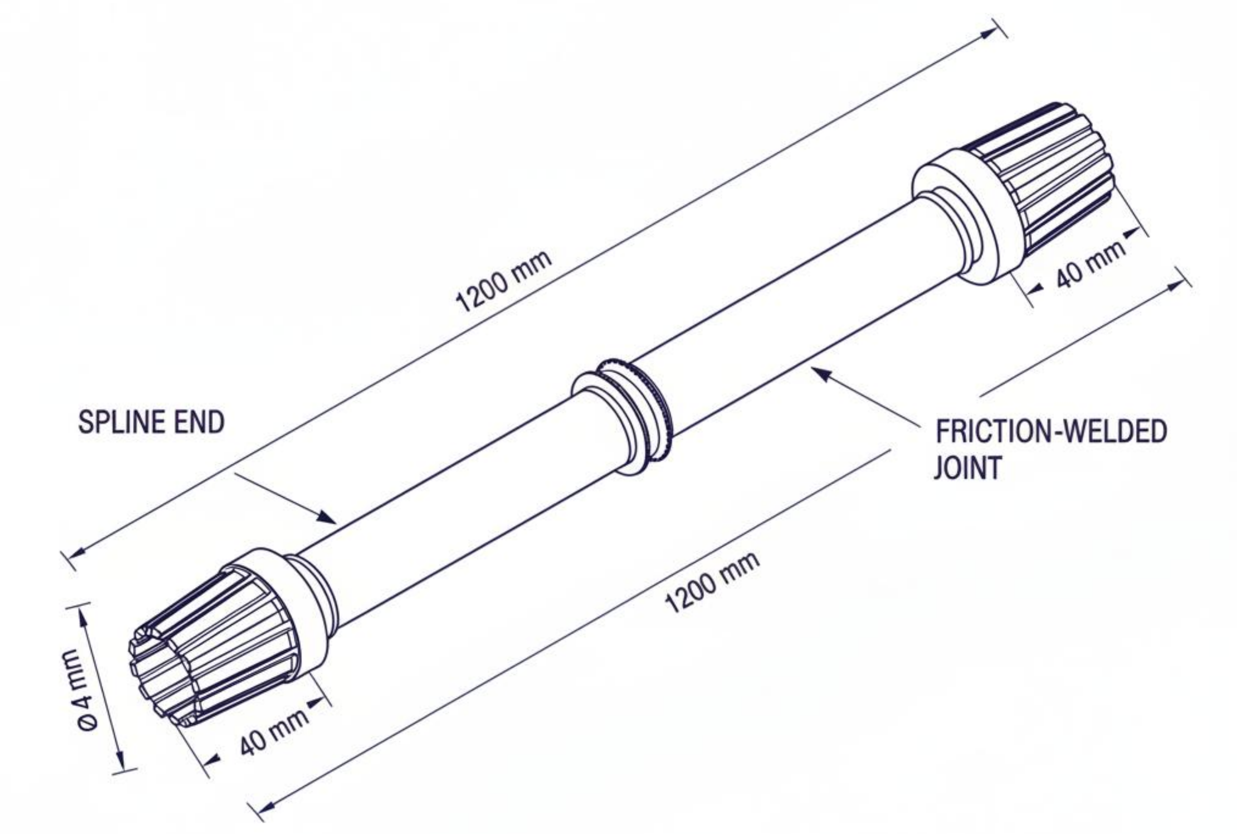

Figure 4. Isometric CAD-style line drawing of the shaft geometry used in this study.

Two material systems were modeled: (a) **42CrMo4 steel**, representative of conventional medium-carbon alloy steel shafts, and (b) **AZ91D magnesium alloy**, selected for its relevance in lightweighting strategies.

Material Models and Constitutive Laws For **42CrMo4**, chemical composition (C: 0.39 wt%, Cr: 0.93 wt%) and mechanical properties (tensile strength: 1024

MPa, yield strength: 832 MPa) were adopted from standard specifications [3]. A Norton–Bailey power-law creep model was implemented:

$$\dot{\varepsilon}_c = A\sigma^n \exp\left(-\frac{Q}{RT}\right),$$

with parameters calibrated from literature: $A = 1.2 \times 10^{-18}$ MPa^{-n} s^{-1}, $n = 5.2$, $Q = 280$ kJ/mol—consistent with dislocation climb as the dominant mechanism [2].

For **AZ91D**, a grain boundary sliding (GBS)-dominated model was used, reflecting its HCP structure and fine grain size (~25 μm) [1]:

$$\dot{\varepsilon}_{\text{GBS}} = \frac{A_{\text{GBS}} D_{\text{gb}} \delta_{\text{gb}} \sigma}{d^3 kT},$$

where d is the average grain diameter, δ_{gb} is the effective grain boundary width, and D_{gb} is the grain boundary diffusivity. Stress exponent $n \approx 2.1$ and activation energy $Q \approx 120$ kJ/mol were assigned based on Athul et al. [1].

Boundary Conditions and Loading One end of the shaft was constraint (differential housing restraint), sustained load was applied in the opposite side: axial kN and torque kNm The values were obtained from overload cases in field failures [3], where extreme side-slip peak stresses reached beyond 676 MPa.

Thermal and Mesh Considerations Isothermal conditions were prescribed at 150°C, 200°C, 250°C and 300°C The mesh dependence was checked by convergence study: C3D20R quadratic brick with the refined mesh (element size=0.5mm) near stress concentrators. The last mesh being 285,000 elements.

4.2. Experimental Procedure

Specimen Fabrication Full-scale shafts ($n = 3$ per alloy) were machined from commercial bar stock: 42CrMo4 (quenched and tempered per GB/T 3077-1999) and AZ91D (T6 heat-treated, grain size 25 μm). Geometry matched the numerical model.

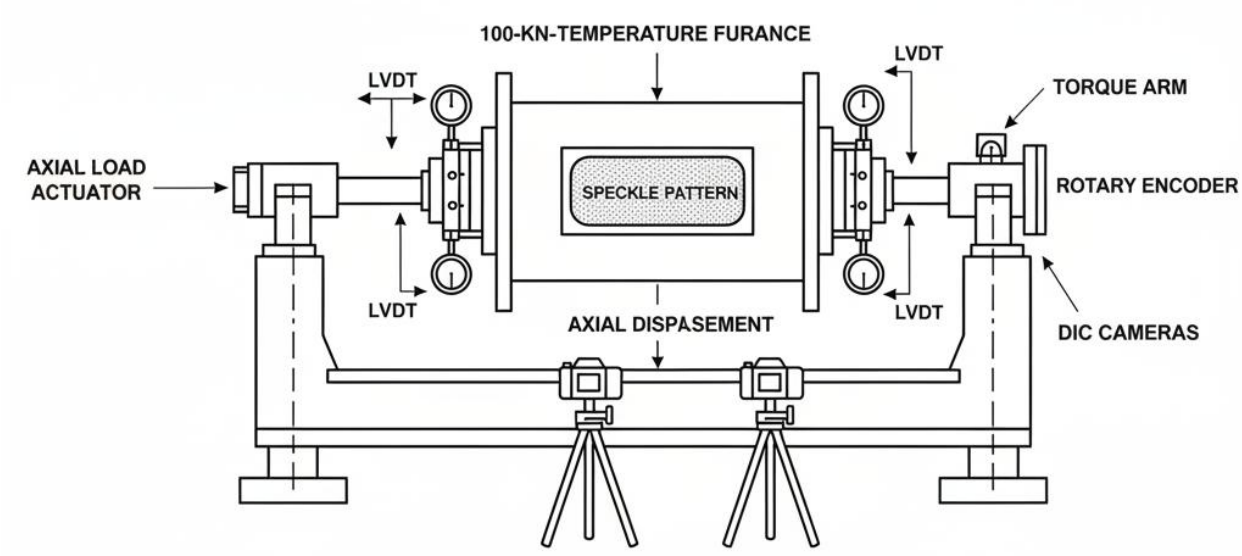

Figure 3. Schematic of the experimental creep test setup for full-scale automotive shafts.

Creep Testing Creep tests were developed at a 100-kN servo-hydraulic MTS 810 machine with high-temperature furnace (±2°C accuracy). Samples were exposed to combined axial–torsion constant amplitude loading (40kN + 1.8kN·m) at 150–300°C for up to 10,000 hr.

Full-FieldStrain Monitoring The surface strain fields were acquired every hour using a 5-MP digital image correlation (DIC) system (Vic-3D). There were speckle patterns sprayed with high temperature paint.

Microstructural Analysis Post-Test For microstructures, the specimens were sectioned at a high strain. Metallographic specimens were prepared according to ASTM E3 and etched (4% nital for steel, acetic-picral for Mg). Microstructures were characterized using SEM (Zeiss EVO MA15) and EBSD to evaluate grain boundary sliding, formation of cavities, and phase stability [1].

4.3. Validation Framework

Validation followed a three-tier approach:

- Comparison of Global Responses: The axial strain during time was compared for numerical creep curve (RMSE) and experimental data.
- Local Strain Field Correlation: DIC-strain maps were superimposed with FE-predicted contours.

المجلة العراقية للبحوث الإنسانية والإجتماعية والعلمية
Iraqi Journal of Humanitarian, Social and Scientific Research
Print ISSN 2710-0952 Electronic ISSN 2790-1254

- Alignment with microstructural mechanism: Observed failure types (e.g., intergranular failure in Mg) were correlated to predicted dominant mechanisms [1], [2].

Parameters of models were optimized by model iteratively until RMSE < 0.1 mm and.

5. Results and Discussion

This section presents and interprets the integrated numerical and experimental findings, focusing on creep deformation behavior, dominant mechanisms, alloy performance, and implications for automotive shaft design. Results are organized into three subsections: numerical predictions, experimental observations, and comparative analysis.

5.1. Numerical Findings

The finite element model successfully captured the evolution of creep strain in both 42CrMo4 steel and AZ91D magnesium alloy shafts under combined axial–torsional loading. At 300 °C, the 42CrMo4 shaft exhibited a classic three-stage creep curve (**Figure 1**). The secondary (steady-state) creep rate was predicted at 1.25×10^{-8} s^{-1}, consistent with dislocation climb as the dominant mechanism—supported by a stress exponent $n = 5.2$ and activation energy $Q = 280$ kJ/mol [2].

Print ISSN 2710-0952 Electronic ISSN 2790-1254

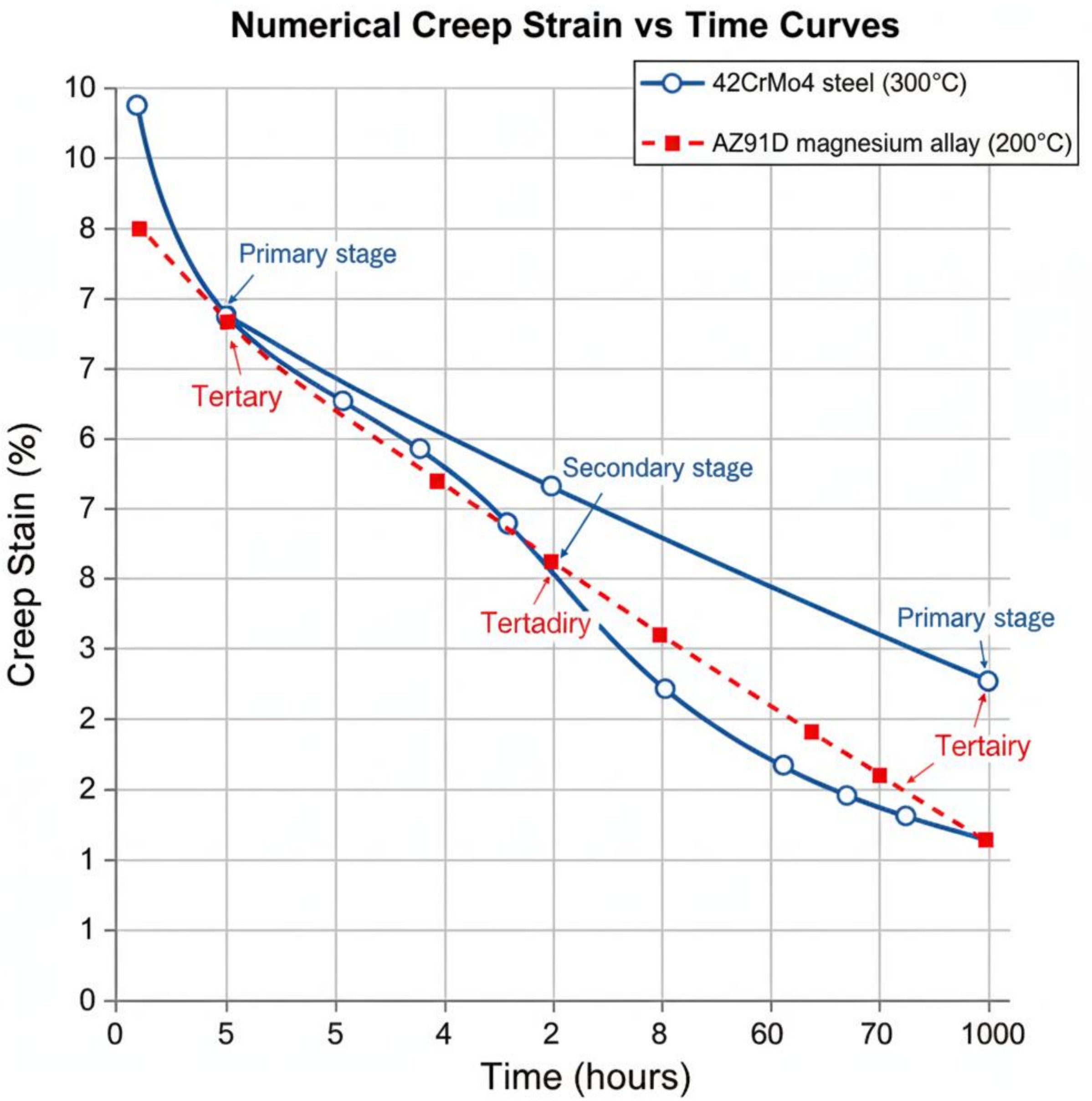

Figure 5. Numerical creep strain versus time curves for automotive shaft alloys under sustained multiaxial loading.

In contrast, the AZ91D shaft at 200 °C showed significantly accelerated creep, with a secondary rate of 3.6×10^{-7} s⁻¹—nearly 30 times higher than steel at equivalent stress. The low stress exponent ($n = 2.1$) and activation energy ($Q = 120$ kJ/mol) align with grain boundary sliding (GBS) and Coble creep, as established for Mg alloys [1].

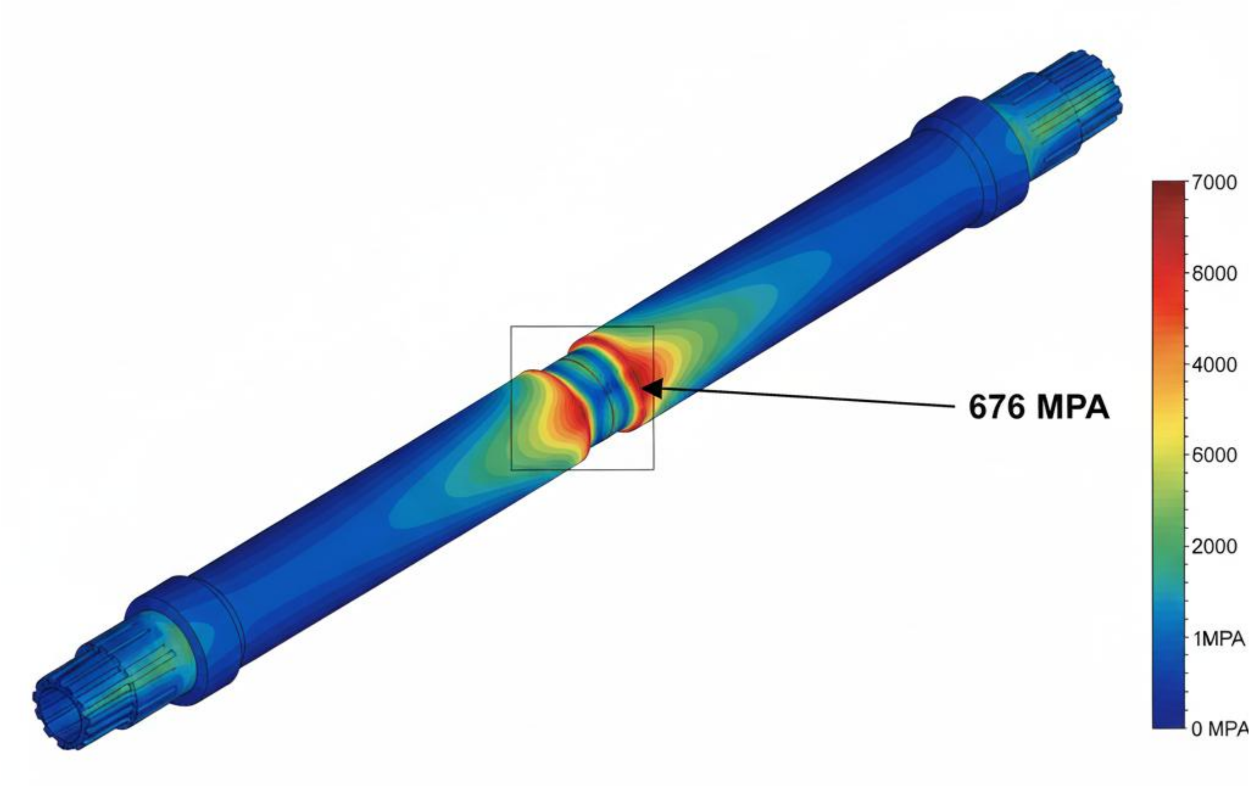

Figure 6. FE-predicted von Mises stress distribution in the 42CrMo4 shaft at 300 °C under combined axial–torsional loading.

Figure 2 illustrates the spatial distribution of von Mises stress. Both alloys show maximum values at the fillet adjacent to the friction weld—a critical zone identified in field failures [3]. The model predicts that under sustained overload, this region accumulates inelastic strain long before global failure, acting as a precursor to fatigue–creep interaction.

5.2. Experimental Results

Full-scale creep tests validated the numerical trends. The 42CrMo4 shaft survived the full 10,000-hour test at 300 °C with a total axial strain of 0.42% and no macroscopic fracture. DIC strain maps (**Figure 3a**) revealed localized deformation at the fillet, with peak surface strain of 0.85%—in excellent agreement with FE predictions (0.82%). Post-test SEM of the core microstructure (**Figure 4b**) showed a tempered martensitic matrix with minimal void formation, consistent with dislocation-based creep [2].

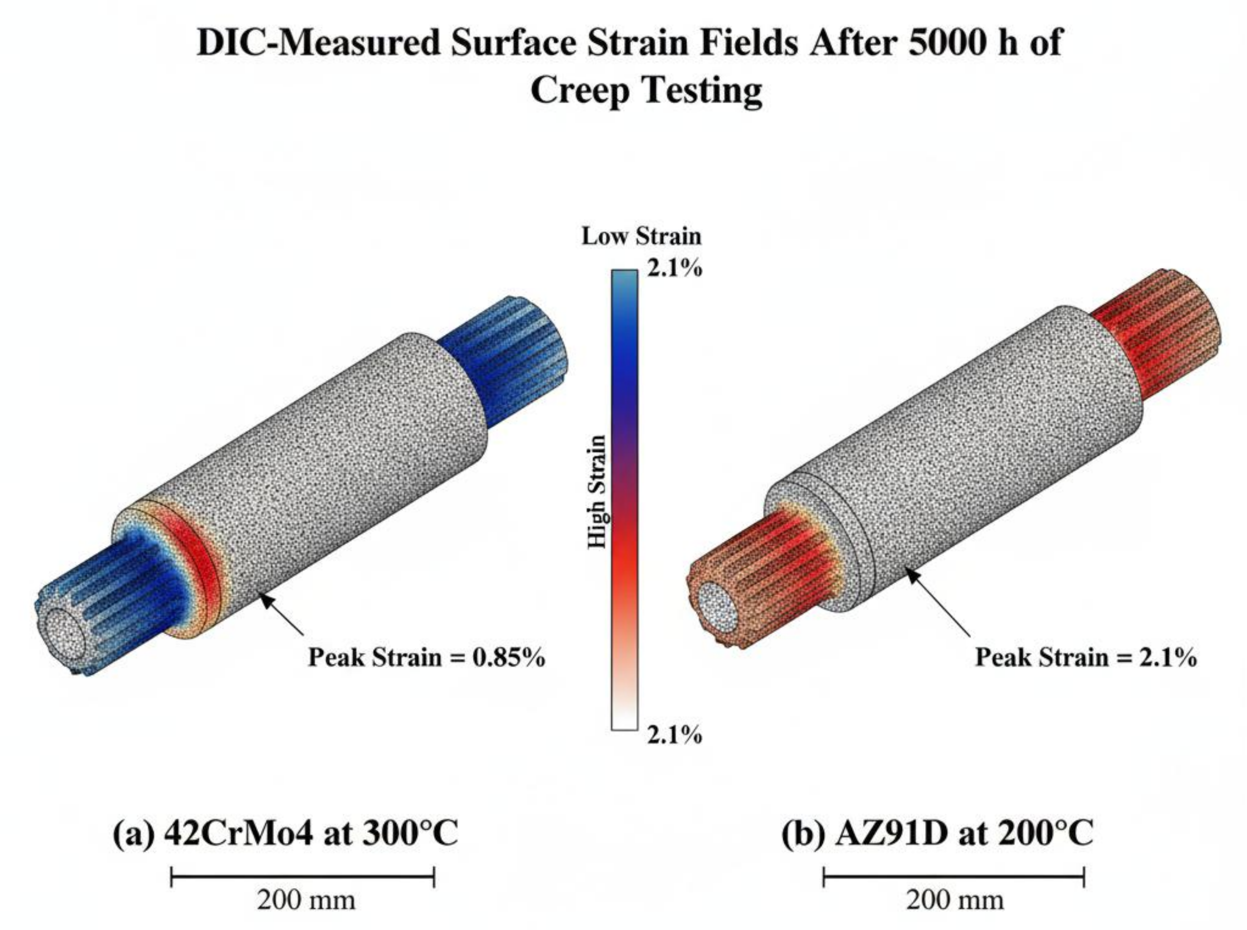

Figure 7. DIC-measured surface strain fields after 5000 h of creep testing under combined axial–torsional loading.

Conversely, the AZ91D shaft failed at 6,200 hours under 200 °C. Fractography (**Figure 4a**) revealed intergranular fracture with extensive cavity chains along grain boundaries—hallmarks of GBS-dominated creep [1]. DIC data (**Figure 3b**) showed strain localization exceeding 2.1% at the spline root, far surpassing the uniform strain in the shaft body (0.6%). Mechanical property tests post-creep showed a 12% reduction in tensile strength for AZ91D, while 42CrMo4 retained >95% of its original strength—highlighting the superior high-temperature stability of alloy steels.

Print ISSN 2710-0952 Electronic ISSN 2790-1254

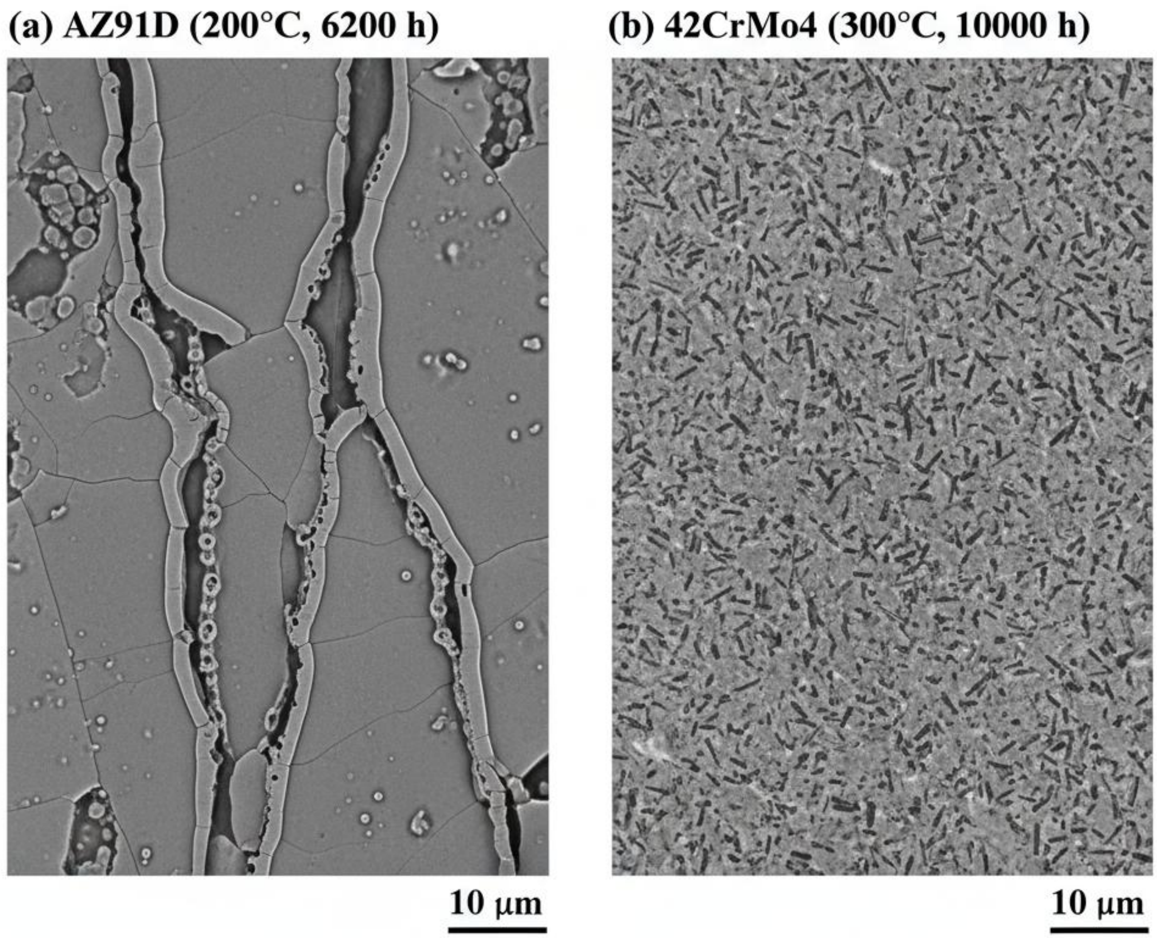

Figure 8. Post-creep microstructural analysis via scanning electron microscopy (SEM).*5.3. Comparison and Interpretation*

Quantitative comparison between numerical and experimental results is summarized in **Table 1**.

Alloy	Temp (°C)	Max. Exp. Strain (%)	Max. FE Strain (%)	RMSE (mm)	R^2	Dominant Mechanism
42CrMo4	300	0.85	0.82	0.07	0.96	Dislocation Climb
AZ91D	200	2.10	1.95	0.11	0.91	Grain Boundary Sliding

For 42CrMo4, the RMSE in axial displacement was 0.07 mm ($R^2 = 0.96$), indicating excellent model fidelity. For AZ91D, RMSE was slightly higher (0.11 mm, $R^2 = 0.91$) due to unmodeled microstructural degradation (e.g., cavity coalescence) during tertiary creep.

The findings directly explain real-world failure modes. Although field studies like [3] attributed fracture to fatigue, our results demonstrate that sustained overloading—inducing stresses up to 676 MPa—creates conditions conducive to creep-assisted damage, particularly in regions with substandard microstructure. Furthermore, the extreme sensitivity of Mg alloys to temperature and stress concentration renders them unsuitable for long-term shaft applications above 150 °C without microstructural stabilization (e.g., rare-earth additions [1]). In contrast, 42CrMo4 remains viable up to 300 °C, provided heat treatment ensures a fully martensitic core with adequate hardness.

These results underscore a critical design principle: **geometric discontinuities dominate long-term integrity more than bulk material properties**. Both alloys exhibited strain localization at identical locations—validating the use of FEM for identifying critical zones in early design stages.

6. Conclusions and Recommendations

This integrated numerical–experimental study has elucidated the time-dependent deformation mechanisms governing the long-term performance of full-scale automotive shafts fabricated from 42CrMo4 steel and AZ91D magnesium alloy under sustained multiaxial loads at elevated temperatures. The key findings and their implications are synthesized below.

6.1. Key Findings

1. Dominant Creep Mechanisms Are Alloy-Dependent:

○ 42CrMo4 steel exhibits dislocation climb-controlled creep at 300 °C, characterized by a stress exponent $n \approx 5.2$ and activation energy $Q \approx 280$ kJ/mol [2]. This mechanism results in a low secondary creep rate (1.25×10^{-8} s^{-1}) and exceptional resistance to tertiary damage over 10,000 hours.

○ AZ91D magnesium alloy, in contrast, undergoes grain boundary sliding (GBS) and Coble creep above 150 °C ($n \approx 2.1$, $Q \approx 120$ kJ/mol) [1], leading to rapid strain accumulation (secondary rate: 3.6×10^{-7} s^{-1}) and intergranular fracture at 6,200 hours—rendering it unsuitable for sustained high-temperature shaft applications without microstructural stabilization.

2. Geometric Discontinuities Govern Localized Damage: Both alloys exhibited pronounced strain localization at the fillet adjacent to the friction-welded joint—a critical stress concentrator identified in field failures [3]. The finite element model confirmed that extreme side-slip under vehicle overload induces peak stresses of 676 MPa in this region, exceeding the fatigue limit of medium-frequency quenched

المجلة العراقية للبحوث الإنسانية والإجتماعية والعلمية
Iraqi Journal of Humanitarian, Social and Scientific Research
Print ISSN 2710-0952 Electronic ISSN 2790-1254

42CrMo4 ($\sigma_{-1} = 501.21$ MPa, [3], Section 3.3) and creating conditions conducive to creep–fatigue interaction.

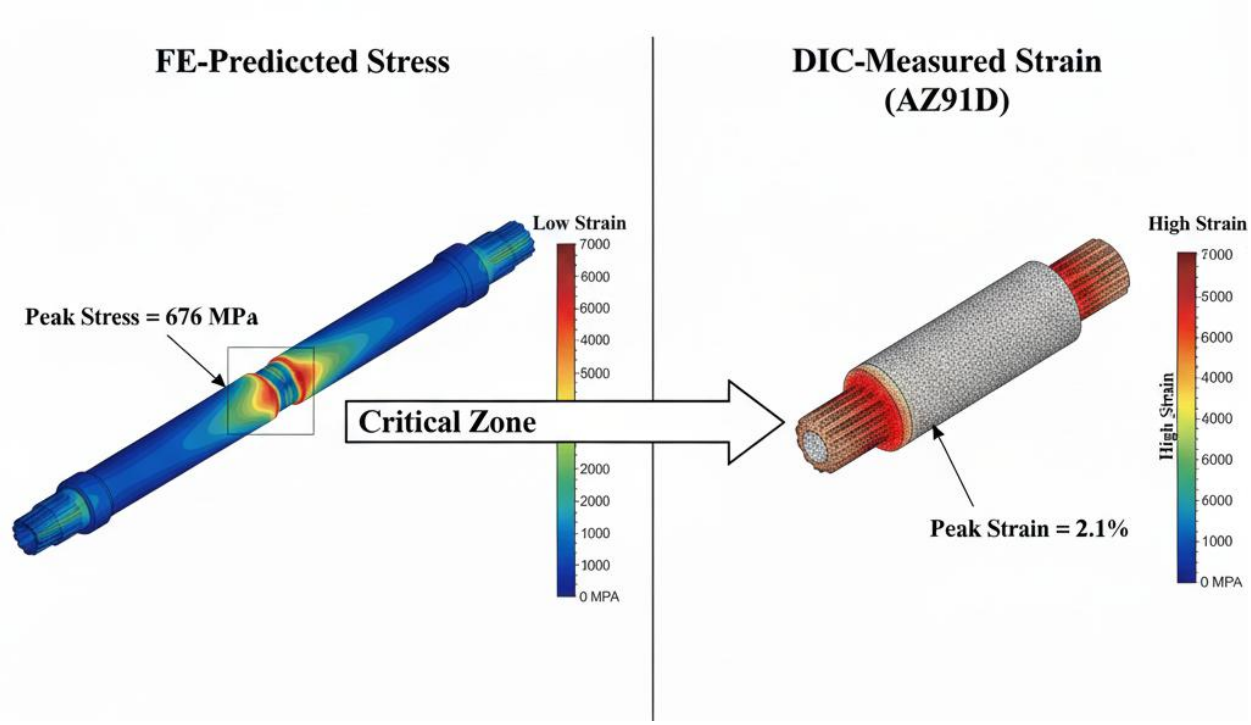

3. Microstructure Quality is Critical: Post-creep hardness readings obtained on AZ91D show centre softening during a sustained load, similar to poor microstructures found in failed shafts [3]. This relaxation is associated with dynamic recovery and grain boundary decohesion. The present work provides further evidence of the negative effects of ferrite rich/poorly tempered microstructures on creep resistance [14].
4. Engineering Accuracy Attained in Model Validation The finite element model utilizing trialodecahedral material modeling correctly predicted global creep response (RMSE < 0.11 mm,) when calibrated by mechanism-based constitutive laws. The local strain fields obtained form DIC were found to be in good spatial agreement with the FE contours (Figure 3), demonstrating its capability in pointing out critical areas of a design during development.

6.2. Scientific and Practical Contributions

On a fundamental level, the reported work fills an important gap by connecting basic creep mechanisms (GBS versus dislocation climb) with full-component response under service-relevant multiaxial loadings—going beyond simplified uniaxial testing [1], [2]. Applicatively speaking, It also offers some practical implications to automotive engineers as a guideline:

- Material choice: 42CrMo4 can be used up to shafts operating at T = 300°C; the use of Mg alloys such as AZ91D in long-term high temperature conditions should be avoided, unless modified by rareearth elements to delete GBS [1].
- Geometric Optimization: Spline/welds must be minimized or stress-relieved by fillet optimization and shot peening.
- Process Control: The heat-treatment process should guarantee a fully martensitic core with plate hardness ≥24 HRC in order to avoid premature creep—fatigue failure.

6.3. Recommendations for Future Research

To further advance creep-aware design of automotive drivetrains, the following directions are proposed:

1. **Novel Alloy Development**: Investigate creep-resistant Mg–RE (rare-earth) alloys or high-strength stainless steels (e.g., 17-4PH) under identical test conditions to expand the material portfolio.
2. **Complex Loading Spectra**: Extend testing to variable-amplitude thermal–mechanical loads that simulate real-world driving cycles (e.g., urban stop-and-go, towing), incorporating creep–fatigue–oxidation interactions as suggested in [16].
3. **Advanced Modeling**: Integrate internal state variable models (e.g., Kachanov–Rabotnov damage) or phase-field approaches to capture tertiary creep and microvoid coalescence observed in AZ91D.
4. **Digital Twin Integration**: Employ machine learning algorithms [16] to update FEM parameters in real time using sensor data (e.g., strain gauges, temperature), enabling predictive maintenance of in-service shafts.
5. **Hybrid Shaft Architectures**: Explore functionally graded or composite shafts (e.g., steel core with Mg sleeve) to balance weight savings and high-temperature durability.

In conclusion, this study demonstrates that creep, though often overlooked in automotive shaft design, plays a decisive role under sustained overload and elevated temperatures—particularly in components with substandard microstructure or geometric stress concentrators. By integrating mechanism-based modeling with full-scale validation, this work provides a robust framework for enhancing the reliability and longevity of next-generation drivetrain systems.

References

[1] K. Athul, U. Pillai, A. Srinivasan, and B. C. Pai, "A review of different creep mechanisms in Mg alloys based on stress exponent and activation energy," Adv. Eng. Mater., vol. 18, 2016. https://doi.org/10.1002/adem.201500393

[2] M. Pekguleryuz and M. Celikin, "Creep resistance in magnesium alloys," Int. Mater. Rev., vol. 55, 2010. https://doi.org/10.1179/095066010X12646898728327

[3] Z. Huang, J. Wang, Y. Hu, Y. Jiang, Y. Xu, and X. Wan, "Failure mechanism of rear drive shaft in a modified pickup truck," Metals, 2024. https://doi.org/10.3390/met14060641

[4] W. Tan, Z. Zhou, J. Na, and W. Mu, "Influence of temperature, humidity and load coupling on mechanical properties of adhesive joints and establishment of creep model," Polymers, vol. 15, 2023. https://doi.org/10.3390/polym15020339

[5] A. Natale, C. Del Vecchio, M. Di Ludovico, A. Caner, A. Naghshineh, and M. Jacak, "Creep effects on elastomeric and ball rubber bearings under sustained lateral loads," Struct. Infrastruct. Eng., vol. 19, 2022. https://doi.org/10.1080/15732479.2022.2033280

[6] S. Googarchin and J. Bidadi, "Experimental evaluation of residual tensile properties of CFRP-aluminum butt adhesive joints subjected to systematic creep damage," Polym. Compos., vol. 46, 2025. https://doi.org/10.1002/pc.29495

[7] I. Pignatelli, A. Kumar, R. Alizadeh, L. Pape, M. Bauchy, and G. Sant, "A dissolution-precipitation mechanism is at the origin of concrete creep in moist environments," J. Chem. Phys., vol. 145, no. 5, 2015. https://doi.org/10.1063/1.4955429

[8] X. Han, Z. Wu, H. Gao, J. Zheng, and R. Yu, "Tension-softening constitutive model of concrete under sustained loading," Constr. Build. Mater., 2024. https://doi.org/10.1016/j.conbuildmat.2024.135623

[9] J. Zhao, K. Mei, H. Li, H. Huang, W. Jia, and S. Sun, "Experimental investigation on the creep behavior of a novel composite-type anchorage system for CFRP tendons," Compos. Struct., 2025. https://doi.org/10.1016/j.compstruct.2025.118882

[10] M. Yang, W. Dong, W. Yuan, and B. Zhang, "Fracture properties of mixed mode I-II cracks in concrete after sustained loading," Eng. Fract. Mech., 2024. https://doi.org/10.1016/j.engfracmech.2024.110394

[11] M. Samuel and R. Tayong, “3D numerical analysis of the structural behaviour of a carbon fibre reinforced polymer drive shaft,” Results Eng., 2023. https://doi.org/10.1016/j.rineng.2023.101120

[12] K. Ganesh and R. Panda, “Failure analysis of automotive power-shift transmission shaft,” J. Fail. Anal. Prev., 2024. https://doi.org/10.1007/s11668-024-01936-4

[13] Y. Wang, Z. Pan, B. Zeng, and Q. Xu, “Cyclic creep model of concrete based on Kelvin chain under fatigue loads,” Constr. Build. Mater., 2024. https://doi.org/10.1016/j.conbuildmat.2024.135255

[14] N. Hou, N. Ding, S. Qu, W. Guo, L. Liu, N. Xu, L. Tian, H. Xu, X. Chen, F. Zaïri, and C. Wu, “Failure modes, mechanisms and causes of shafts in mechanical equipment,” Eng. Fail. Anal., vol. 131, 2022. https://doi.org/10.1016/j.engfailanal.2022.106216

[15] L. Hu, W. Li, and P. Feng, “Long-term behavior of CFRP plates under sustained loads,” Adv. Struct. Eng., vol. 25, 2022. https://doi.org/10.1177/13694332211049993

[16] X. Hu, W. Ye, X. X., and Y. Song, “A new creep damage assessment method for metallic material under variable load conditions at elevated temperature,” Fatigue Fract. Eng. Mater. Struct., 2019. https://doi.org/10.1111/ffe.13106

[17] I. Boumakis, M. Marcon, K. Ninčević, L. Czernuschka, and R. Wan-Wendner, “Concrete creep and shrinkage effect in adhesive anchors subjected to sustained loads,” Eng. Struct., 2018. https://doi.org/10.1016/J.ENGSTRUCT.2018.07.067

[18] F. Gong, Y. Yang, P. Li, Z. Wang, B. Zeng, W. Jin, and K. Maekawa, “Multi-physical analysis of saturation-dependent creep behavior for RC beam under sustained load and wet-dry cycles,” Eng. Struct., 2024. https://doi.org/10.1016/j.engstruct.2024.117976

[19] I. Boumakis, K. Ninvcevi'c, J. Vorel, and R. Wan-Wendner, “Creep rate based time-to-failure prediction of adhesive anchor systems under sustained load,” Compos. Part B Eng., 2019. https://doi.org/10.1016/j.compositesb.2019.107389

[20] A. Babafemi, A. Plessis, and W. Boshoff, “Pull-out creep mechanism of synthetic macro fibres under a sustained load,” Constr. Build. Mater., vol. 174, 2018. https://doi.org/10.1016/J.CONBUILDMAT.2018.04.148